International Journal of Heat and Technology
Vol. 36, No. 4, December, 2018, pp. 1510-1516
Journal homepage: http://iieta.org/Journals/IJHT

Optimization of deployment pattern parameters of horizontal well fracturing in tight oil reservoirs

Linjing Xu[1,3]*, Guoyong Wang[1], Tianyu Liu[2], Naizhen Liu[1], Shicheng Zhang[3], Tingshuai Zhang[1]

[1] CNPC Great Wall Drilling Company, Beijing 100101, China
[2] Oil & Gas Field Development Institute, Research Institute of Petroleum Exploration and Development, Beijing 100083, China
[3] Lab of Petroleum Eng. of MOE, China University of Petroleum, Beijing 102249, China

Corresponding Author Email: xiaoba103@126.com

https://doi.org/10.18280/ijht.360445

Received: 2 March 2018
Accepted: 1 June 2018

Keywords:
horizontal well fracturing (HWF), injection well, production well, tight oil reservoir, well spacing

ABSTRACT

This paper establishes a new numerical simulation model for the two-phase coupled flow in tight oil reservoir: the complex fractures in near-well region are described by a dual-porosity model, while those in far-field region are illustrated by a single-porosity model. Then, a pressure displacement system was created between the injection and production wells to effectively drain the reservoir stratum. After that, the productivity and seepage features of the wells were studied under different well patterns, while the fracturing parameters of injection wells were examined by the simulation model. The research results show that the injection at 100m away from the simulated reservoir volume (SRV) region has minimal impact on tight oil production; the injection wells should be deployed on the edge of the maximum drainage area, aiming to replenish the near-well zone with far-field fluid; more injection wells in the SRV region of tight oil reservoir does not mean better yield.

1. INTRODUCTION

Since its birth in 1985, horizontal well fracturing (HWF) has been extensively studied and constantly improved, creating cutting edge techniques like horizontal well volume fracturing (HWVF). Under different assumptions and seepage principles, various productivity formulas have been derived by conformal transformation method [1], equivalent seepage resistance method [2], complex potential theory, and superposition principle [3]. Since most oil reservoirs have similar seepage features, the previous studies on the HWF often simulate the reservoir conditions as simple, elliptical models. Under stable Darcy flow, hydraulic fractures exhibit infinite fracture conductivity [4] or act as a semi-analytical model [5-6]. Obvious, the above HWF models fail to consider the geological or seepage field features after fracturing treatment in tight oil reservoirs, which is a global hotspot of oil development.

In recent years, horizontal wells have been applied to tight oil exploitation, yielding certain achievements [7]. The fractures formed in the HWF serve as oil channels, which increases the drainage and productivity of a single well. Specifically, injection wells are deployed around each production well to form a well pattern. Together, the injection wells maintain the formation pressure needed for oil production, pushing up the production yield and efficiency of the production well. However, the research on the pattern of horizontal wells is in its infancy, calling for proper optimization of the relevant parameters. Ranging from well pattern, fracture shape to well length, these parameters are closely correlated and mutually interfering. It is impossible to disclose their impacts on horizontal well productivity by traditional single-parameter analysis [8~11]. The qualitative analysis may be a viable solution to identify the said impacts, laying the basis for HWF deployment and support. In addition, the previous studies [12-13] have proved recovery degree as a key determinant of horizontal well pattern.

As an emerging HWF method, synchronous fracturing refers to the simultaneous fracturing in two horizontal wells, whose fracturing sections are designed preliminarily at the beginning. During the fracturing, the stress turning radius is reduced by the superposition effect of the stress field near the tip of fracture. In this way, the new fractures will initiate in a close range [14-15]. Compared with single-well fracturing, the synchronous fracturing allows fractures to propagate in opposite directions. In this case, the normal stress at the fracture end changes slightly, but the shear stress near the fracture tip undergo significant changes. Besides, the tensile and shear stresses increase as the opposite propagation continues [16]. Since the stress disturbance is limited to the facture tip, the inter-well connectivity may be adopted in actual construction to improve the fracturing section and sequence of adjacent wells, considering the major impacts of well spacing and fracture length on stress disturbance.

Considering the above, this paper establishes a new numerical simulation model for the two-phase coupled flow in tight oil reservoir: the complex fractures in near-well region are described by a dual-porosity model, while those in far-field region are illustrated by a single-porosity model. Then, a pressure displacement system was created between the injection and production wells to effectively drain the reservoir stratum. After that, the productivity and seepage features of the wells were studied under different well patterns, while the fracturing parameters of injection wells were examined by the simulation model.

2. MODEL DESCRIPTION

2.1 Mathematical formulation

(1) Near-well reservoir (dual-porosity zone)

The Warren-Root dual-porosity model [13] was adopted to simulate the flow in the fracture system. The reservoir was modelled as two overlapping continua, namely, the fracture system and the matrix system. The interaction between the two continua is controlled by a transfer factor α. The reservoir model is subjected to the following hypothesis: the model is a 3D representation of a two-phase (oil and water) flow; the start-up the two-phase flow is a non-Darcy one, considering only the initial pressure gradient of the oil phase; the permeability and porosity change with the formation pressure; the reservoir fluid is compressible with constant compressibility factors; the gravity is negligible; the bottom hole pressure remains constant. The relevant formulas of the model are as follows:

Oil phase:

$$\nabla[\rho_o \frac{k_m k_{ro}}{\mu_g}(\nabla p_m - G_o)] + \frac{\alpha\rho_o k_m k_{ro}}{\mu_o}(P_{sf} - P_m) = \frac{\partial(\rho_o s_o \phi)}{\partial t} \quad (1)$$

Water phase:

$$\nabla[\rho_w \frac{k_m k_{rw}}{\mu_w}(\nabla P_m - G_w)] + \frac{\alpha\rho_w k_m k_{rw}}{\mu_w}(P_{sf} - P_m) = \frac{\partial(\rho_w s_w \phi)}{\partial t} \quad (2)$$

Oil phase:

$$\nabla[\rho_o \frac{k_{sf} k_{ro}}{\mu_o}\nabla p_{sf}] + \frac{\alpha\rho_o k_m k_{ro}}{\mu_o}(P_m - P_{sf}) = \frac{\partial(\rho_o s_o \phi)}{\partial t} \quad (3)$$

Water phase:

$$\nabla[\rho_w \frac{k_{sf} k_{rw}}{\mu_w}\nabla p_{sf}] + \frac{\alpha\rho_w k_m k_{rw}}{\mu_w}(P_m - P_{sf}) = \frac{\partial(\rho_w s_w \phi)}{\partial t} \quad (4)$$

where

$$G_o = a\left(\frac{K}{\mu_o}\right)^{-b}, \quad K = K_0 e^{[\alpha(P-P_0)]} \text{ and } \phi = \phi_0 e^{[\beta(p-p_0)]} \quad (5)$$

The subscript f is the fracture system; m is the matrix system; P is the fracture system pressure; P_o is the initial pressure of the reservoir; σ is a shape-dependent constant; ρ_o is oil density; ρ_w is water density; k_{sf} is fracture system permeability; k_{ro} is oil relative permeability; k_{rw} is water relative permeability; μ_w is acid viscosity; μ_o is oil viscosity; S_o is oil saturation; S_w is water saturation; φ is porosity; G is the initial pressure gradient; *a* and *b* are regression coefficients; α and β are permeability and porosity coefficients that change with the reservoir pressure (1/MPa). All the parameters are in standard international unit.

(2) Main fractures [14]

The main fractures were simulated under the following assumptions: the model is a 2D representation of a two-phase (oil and water) flow; the fracture is cubic and develops in the vertical direction; the fracture flow obeys the Darcy's law; the flow conductivity varies with time.

The two-phase flow flows linearly from the dual-porosity zone to the main fractures, and then into the wellbore. The seepage control differential equation of the main factures can be expressed as:

$$-\frac{\partial}{\partial x}(\rho_o V_o) - 2\frac{\rho_o V_{y,o}}{W} = \frac{\partial}{\partial t}(\rho_o \phi S_o) \quad (6)$$

where the dynamic fracture permeability K_f is

$$K_f = K_{f0}\exp(-ct) + K_0 \quad (7)$$

K_{fo} is the initial fracture permeability; K_o is the initial formation permeability (μm^2); t is time (d); c is the corresponding regression coefficient.

(3) Far-field reservoir

The far-field reservoir in our model is a single-porosity, 2D linear reservoir. The flow from the far-field single-porosity reservoir into the near-well reservoir is governed by the following partial differential equation.

Oil phase:

$$\nabla[\rho_o \frac{k_m k_{ro}}{\mu_o}(\nabla p_m - G_o)] = \frac{\partial(\rho_o s_o \phi)}{\partial t} \quad (8)$$

Water phase:

$$\nabla[\rho_w \frac{k_m k_{rw}}{\mu_w}(\nabla P_m - G_w)] = \frac{\partial(\rho_w s_w \phi)}{\partial t} \quad (9)$$

2.2 Model solution

Equations (1)~(9) constitute a complete mathematical model for the non-Darcy flow in tight oil reservoir. The reservoir model and the fracture model were solved separately by the implicit pressure, explicit saturations (IMPES) method. The seven diagonal linear equations were processed by conjugate gradient method. During the computation, the time step was selected automatically to improve the convergence rate.

2.3 Model description

The basic data of a tight oil reservoir (Table 1) were adopted to verify the effectiveness of the above mathematical model. The 900,000 m^3 reservoir is a cuboid with a side length of 1,500m, 600m and 10m in x, y and z directions, respectively. With a 1,000m-long shaft, a horizontal well is in the x direction at the center of the reservoir. The reservoir was meshed into 150×60×1 grids, each of which is 10m in size. The half-fracture length was set to 200m, the simulated reservoir volume (SRV) to 4,000,000m^2, and the reservoir area coefficient to 44.4%.

Table 1. Simulation parameters

Parameter	Value	Parameter	Value
Matrix system permeability ($10^{-3}\mu m^2$)	0.1	Oil volume factor (m^3/m^3)	1.5857
Micro-fracture permeability ($10^{-3}\mu m^2$)	30	Oil compressibility (1/MPa)	0.002243
Matrix system porosity (%)	8	Water compressibility (1/MPa)	0. 000486
Micro-fracture porosity (%)	0.3	Rock compressibility (1/MPa)	0.004
Initial water saturation (%)	50.9	Reservoir pressure (MPa)	31.58
Water viscosity (mPa·s)	0.4	Bottom hole pressure (MPa)	20
Oil viscosity (mPa·s)	3.3	Well bore radius (m)	0.1

3. OPTIMIZATION OF WELL PATTERN AND WELL SPACING

In synchronous fracturing, the well spacing is limited by the fracture length, which is usually very long. In this case, it is impossible to adopt the conventional well pattern. Here, vertical injection wells are deployed in different patterns around the horizontal production well, considering the seepage and productivity features as well as the fracture distribution in different displacement systems. Then, the most rational well pattern and was determined by comparing the productivity and displacement effects.

As shown in Figure 1, well spacing refers to the distance between wells and array spacing refers to the distance between the edge of injection well and the outer boundary of the fracturing region. The SRV region in Figure 2 shows that the wells were deployed on the outer edge of the reconstruction region. Next, the author analyzed the impacts of different well spacing and array space on well pattern productivity in tight oil reservoir.

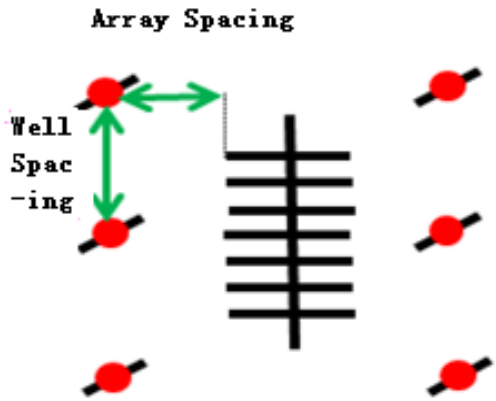

Figure 1. Well pattern

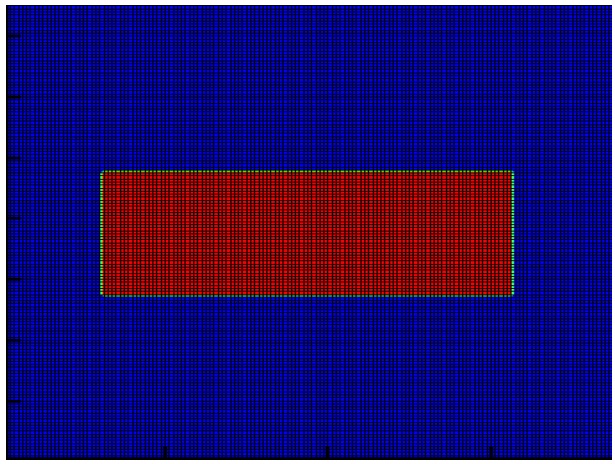

Figure 2. Schematic of SRV

3.1 Production and drainage scope under the same well spacing and different array spacings

(1) Well spacing of 400m and array spacing of 100 m

Case 1: With injection wells

Figure 3 and 4 respectively display the pressure and saturation distributions after 1,000 days of injection at the well spacing of 400m and array spacing of 100m. It is clear that the pressure drainage scope was very small outside the SRV region, and the injected water in the well did not enter the SRV region.

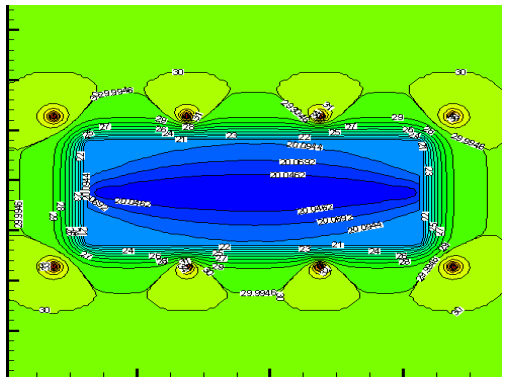

Figure 3. Pressure distribution after 1,000 days of injection at the well spacing of 400m and array spacing of 100m

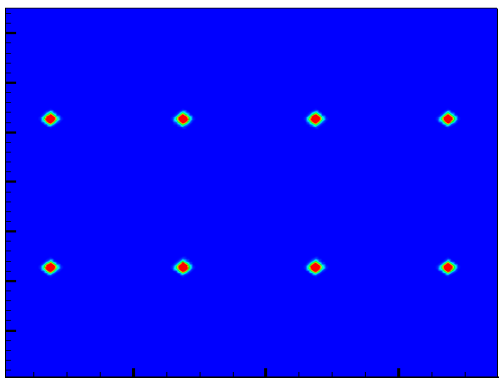

Figure 4. Saturation distribution after 1,000 days of injection at the well spacing of 400m and array spacing of 100m

Case 2: Without injection well

Figure 5 compares the pressure distributions between injection well pattern and depletion development at the array spacing of 100m. Under the presence of an injection well, the cumulative oil production was greater than that of depletion development. This means the pressure had a minimal effect on oil production although the said injection well did not inject water into the SRV region. Hence, the deployment of injection wells within100m away from the SRV region has not major impact on the production of tight oil reservoir, which promotes the optimization of the oil drainage area.

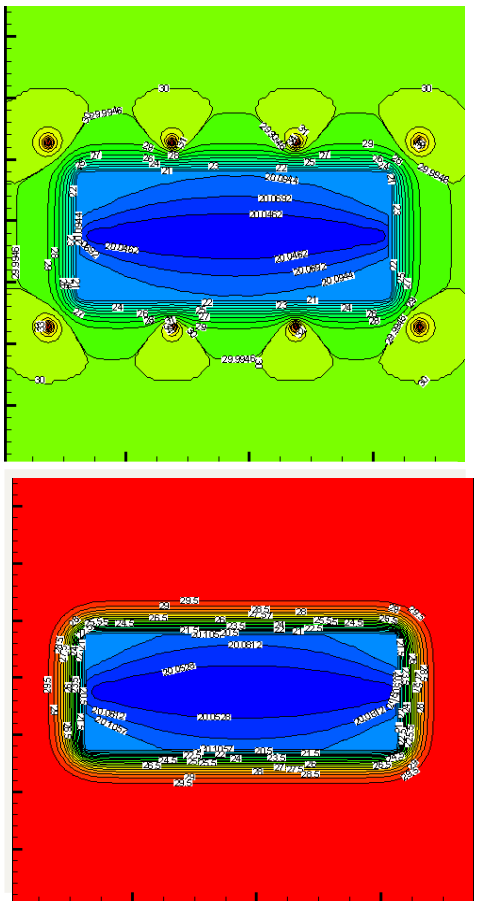

Figure 5. Pressure distribution at the well distance of 100m

(2) Well spacing of 400m and array spacing of 50 m

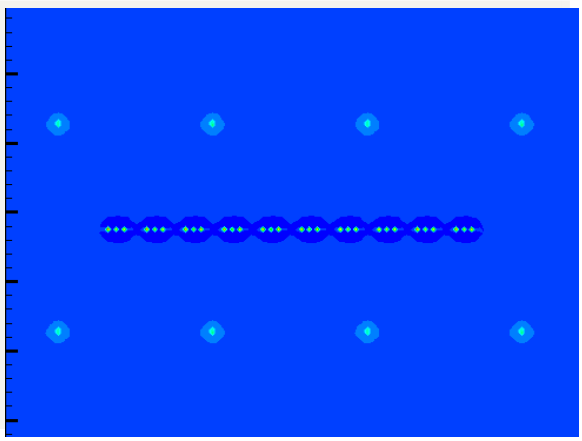

Figure 6. Well pattern development

Figure 6 shows the injection well pattern development on the edge of the SRV region at the well spacing of 400m and the array spacing of 50m. The horizontal well is 1,000m in length and has ten stages. the ten stages of the evolution of a 1,000m long horizontal well, surrounded by two injection wells, on the boundary of the SRV region at the well spacing at 400m and array spacing of 50m, while Figure 7 presents the saturation distribution after 1,000 days of injection at the same distance parameters. It can be seen that the water injection in the middle of the horizontal well was affected, yet the injected water did not affect the SRV region. This is because both sides of the well were at 100m outside the SRV region. Figure 8 describes the pressure distribution at the same distance parameters, also after 1,000 days of injection. Obviously, the pressure affected the area outside the SRV region, indicating that the well should be deployed on the edge of the most severely affected area. Figures 9 and 10 compare the time-varying curves of daily oil production and cumulative oil production in depletion development and the presence of an injection well. With the array spacing of 100m, the daily oil production and cumulative oil production in the presence of injection well were considerably higher than those in depletion development. Therefore, the most effectively way to deploy injection wells in tight oil reservoir is to deploy them on the edge of the SRV region.

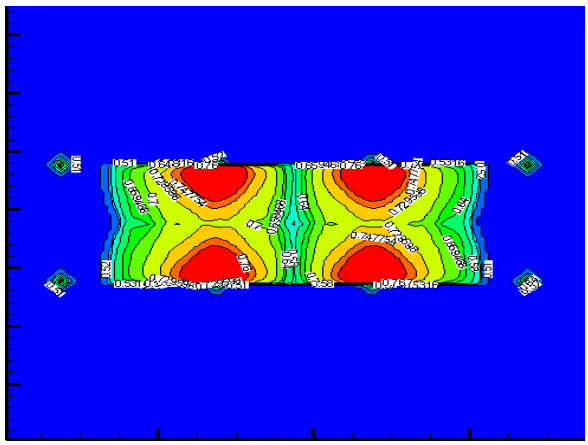

Figure 7. Saturation distribution after 1,000 days of injection at the well spacing of 400m and array spacing of 50m

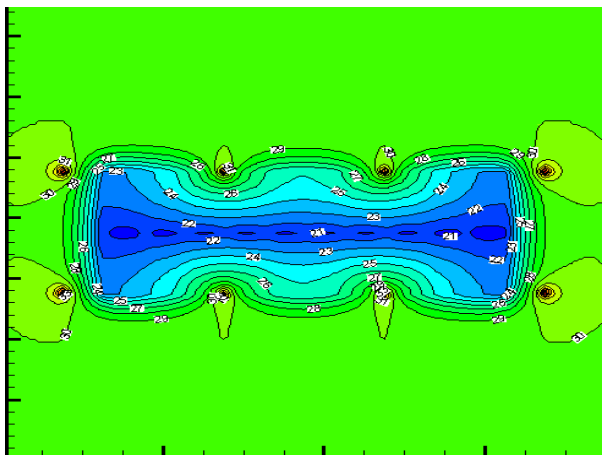

Figure 8. Pressure distribution after 1,000 days of injection at the well spacing of 400m and array spacing of 50m

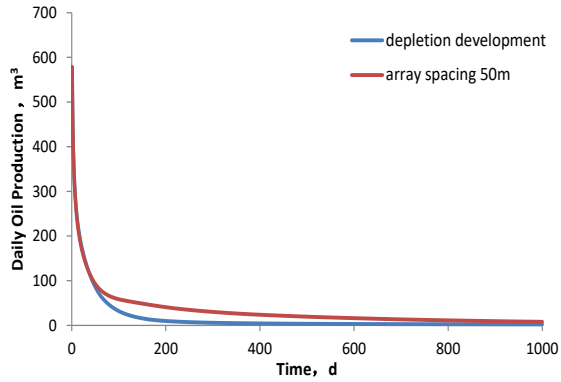

Figure 9. Daily oil productions in the presence of injection wells and depletion development

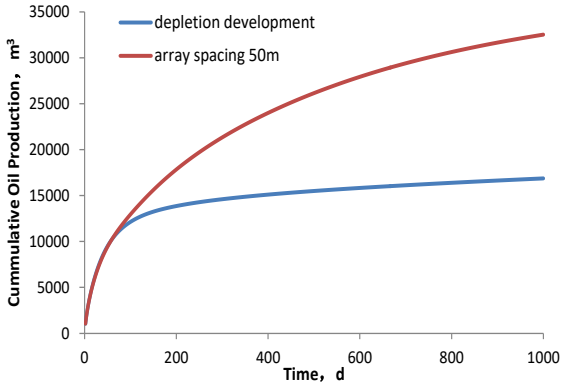

Figure 10. Cumulative oil productions in the presence of injection wells and depletion development

3.2 Production and drainage scope under the same array spacing and different well spacings

If deployed too far away from the SRV region, the injection well cannot play an important role in well stimulation. Thus, well spacing was optimized mostly in the SRV region for tight oil reservoirs.

(1) Array spacing of 50m and well spacing of 200, 300, and 400m

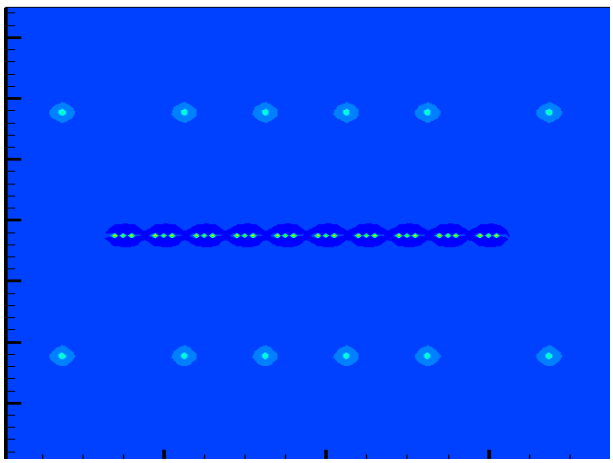

Figure 10. Well pattern development at the well spacing of 200m

Figures 11~13 show the injection well pattern development on the edge of the SRV region at the well spacing of 200, 300 and 400m, respectively. The horizontal well is 1,000m in length and has ten stages. The fracturing was performed at the well spacing of 400m and the array spacing of 50m.

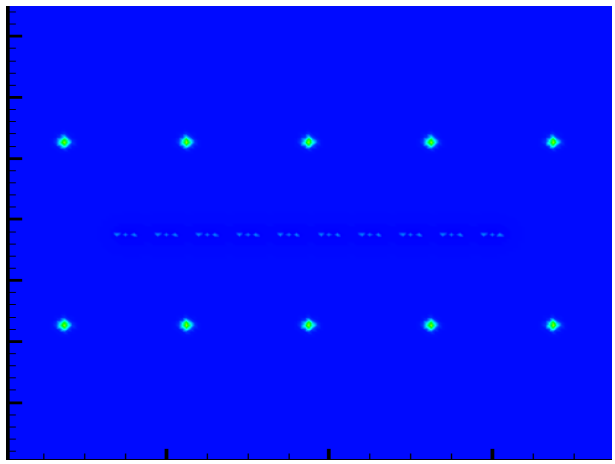

Figure 11. Well pattern development at the well spacing of 300m

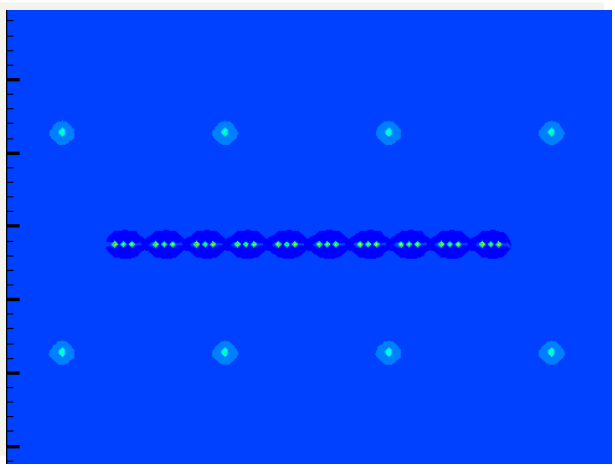

Figure 12. Well pattern development at the well spacing of 400m

(2) Well spacing optimization

Figures 13~15 display the daily oil production, cumulative oil production, and water production at different well spacing, respectively. The results show that the water production was similar at different well spacing initially, and increased with the water flow over time. The water production of 98% was taken as the termination condition of the simulation. The 12 injection wells all witnessed excessively high water production. By oil production, the well spacing were ranked as 400m>300m>200m. Hence, more injection wells in the SRV region of tight oil reservoir does not mean better yield. As the permeability of the SRV region continues to improve, rapid flooding will occur easily if there are too many wells.

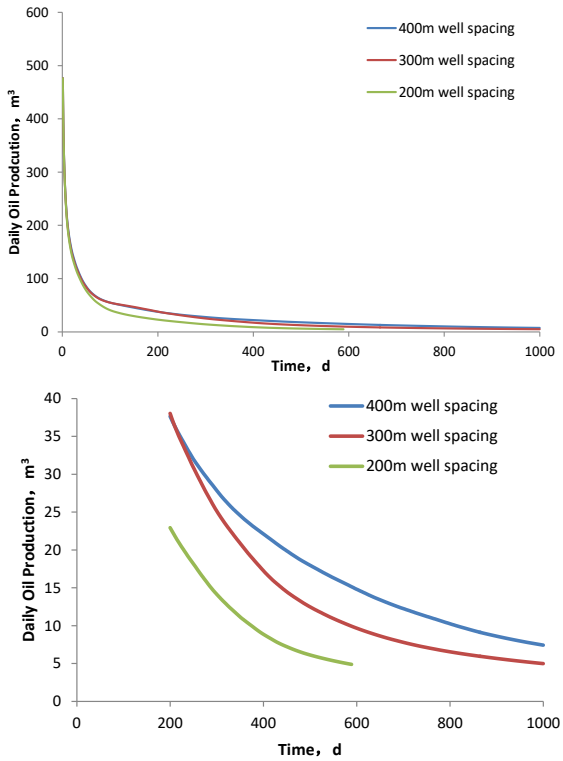

Figure 13. Time variation in daily oil production

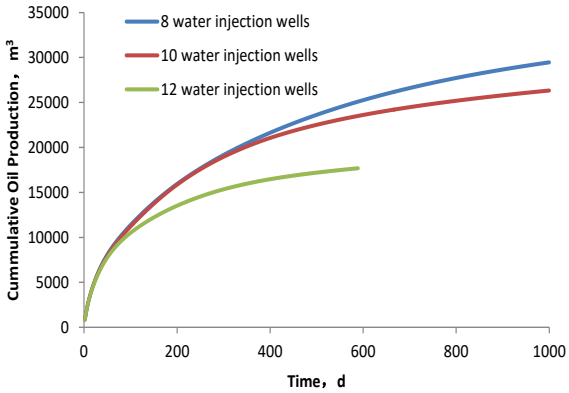

Figure 14. Time variation in cumulative oil production

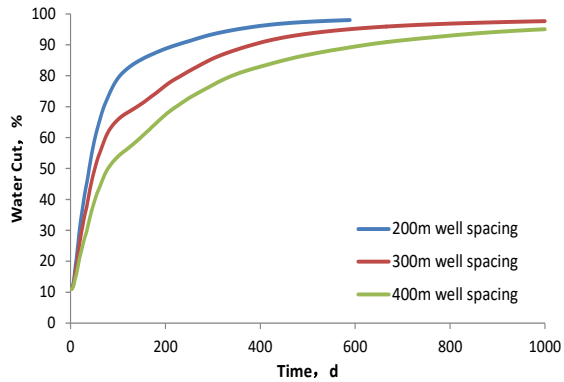

Figure 15. Time variation in water production

4. CONCLUSIONS

Based on the previous results on the effects of single horizontal well on drainage area, this paper carries out a preliminary study on the injection wells of the HWVF technique in tight oil reservoirs, and analyzes the optimal match between injection wells and multi-stage horizontal well. The main conclusions are as follows:

In tight oil reservoirs, the well pattern with array spacing of 100m differs slightly from depletion development in cumulative oil production, revealing that the injection at 100m away from the SRV region has minimal impact on tight oil production.

The target tight oil reservoir was effectively developed when the injection wells were deployed at 50m from the SRV region. Therefore, the injection wells should be deployed on the edge of the maximum drainage area, aiming to replenish the near-well zone with far-field fluid.

More injection wells in the SRV region of tight oil reservoir does not mean better yield. As the permeability of the SRV region continues to improve, rapid flooding will occur easily if there are too many wells.

REFERENCE

[1] Karcher BJ, Giger FM, Combe J. (1986). Some practical formulas to predict horizontal well behavior. SPE Annual Technical Conference and Exhibition. https://doi.org/10.2118/15430-MS

[2] Giger FM, Reiss LH, Jourdan AP. (1984). The reservoir engineering aspects of horizontal drilling. SPE Annual Technical Conference and Exhibition. https://doi.org/10.2118/13024-MS

[3] Joshi SD. (1986). Augmentation of well productivity with slant and horizontal wells. SPE Annual Technical Conference and Exhibition. https://doi.org/10.2118/15375-MS

[4] Economides MJ, Wood DA. (2009). The state of natural gas. Journal of Natural Gas Science and Engineering 1(1-2): 1-13. https://doi.org/10.1016/j.jngse.2009.03.005

[5] Guo B, Schechter DS. (1997). A simple and rigorous mathematical model for estimating inflow performance of wells intersecting long fractures. SPE Asia Pacific Oil and Gas Conference and Exhibition. https://doi.org/10.2118/38104-MS

[6] Wei Y, Economides MJ. (2005). Transverse hydraulic fractures from a horizontal well. SPE Annual Technical Conference and Exhibition. https://doi.org/10.2118/94671-MS

[7] Buffington N, Kellner J, King JG, David BL, Demarchos AS, Shepard LR. (2010). New technology in the Bakken play increases the number of stages in packer/sleeve completions. SPE Western Regional Meeting. https://doi.org/10.2118/133540-MS

[8] Rueda JI, Rahim Z, Holditch SA. (1994). Using a mixed integer linear programming technique to optimize a fracture treatment design. SPE Eastern Regional Meeting. https://doi.org/10.2118/29184-MS

[9] Li XP. (1996). Fluid flow through pay zones in relation to draw-down profiles in a horizontal well intersecting several vertical fractures. Acta Petrolei Sinica 17(2): 91-97. https://doi.org/10.7623/syxb199602014

[10] Lee SH, Jensen CL, Lough MF. (1999). An efficient finite difference model for flowing reservoir with multiple length-scale fractures. SPE Annual Technical Conference and Exhibition.

https://doi.org/10.2118/56752-MS
[11] Williams ET, Kikani J. (1990). Pressure transient analysis of horizontal wells in a naturally fractured reservoir. SPE Annual Technical Conference and Exhibition. https://doi.org/10.2118/20612-MS
[12] Carvalho RSD, Rosa AJ. (1988). Transient pressure behavior for horizontal wells in naturally fractured reservoir. SPE Annual Technical Conference and Exhibition. https://doi.org/10.2118/18302-MS
[13] Yin GF, Xu HM, Ye SJ, Li YR, Qiu JP. (2011). Productivity evaluation model for infill horizontal well in horizontal injection and production pattern. Journal of China University of Petroleum (Edition of Natural Science) 35(4): 93-97. https://doi.org/10.3969/j.issn.1673-5005.2011.04.017
[14] Lutz JF, Kemper WD. (1959). Intrinsic permeability of clay as affected by clay-water interaction. Soil Science 88(2): 83-90. https://doi.org/10.1097/00010694-195988020-00005
[15] Miller RJ, Low PF. (1963). Threshold gradient for water flow in clay systems. Soil Science Society of America Proceedings 27(6): 605-609. https://doi.org/10.2136/sssaj1963.03615995002700060013x
[16] Samaniego VF, Cinco LH. (1980). Production rate decline in pressure-sensitive reservoirs. JCPT 19(3): 75-86. https://doi.org/10.2118/80-03-03